Stochastic Environmental Research and Risk Assessment 15 (2001) 357–371 © Springer-Verlag 2001

A fractal-multifractal approach to groundwater contamination. 1. Modeling conservative tracers at the Borden site

C. E. Puente, O. Robayo, M. C. Díaz, B. Sivakumar

Abstract. The possibility of modeling the dynamics of groundwater contamination plumes using a deterministic fractal-multifractal (FM) approach, via projections off fractal interpolating functions, is investigated. To this effect, the movement of chloride and bromide tracers gathered at the Borden site in Ontario, Canada, during the period August 1982 to June 1985, is studied. Results indicate that the FM methodology provides very faithful and compact geometric descriptions of the contamination process, as the approach captures the (vertically-averaged) two-dimensional patterns of the tracers, both in their low order moments and in their (non-elliptical) geometric shapes. It is shown that the FM approach leads to noticeable trends in "surrogate" (fractal) parameter space that allow viewing the plume's evolution in a simple and wholistic fashion.

1 Introduction

Understanding the dynamics of pollutants in groundwater constitutes one of the most important problems in hydrology. During the past few decades, a large number of studies have attempted to address this problem, resulting in a wide variety of approaches and models.

The classical descriptions of flow and transport in porous media rely on the use of coupled sets of partial differential equations describing the processes. Even though such representations are based on sound physical principles, e.g. conservation laws, their use in practice is often restricted by our inability to measure data at appropriate spatial scales and at desired sampling frequencies. In practical situations, the partial knowledge of relevant "details," for example, (1) initial and boundary conditions; and (2) parameters that reflect non-trivial medium heterogeneities, often results in approximate solutions, which smooth nature's geometries and, hence, distort the observed shape of a plume. The typically intricate soil heterogeneity also prevents us from adequately transferring infor-

C. E. Puente (✉), O. Robayo, M. C. Díaz, B. Sivakumar
Department of Land, Air, and Water Resources,
University of California, Davis, CA 95616, USA
Fax: 530-752-5262
e-mail: cepuente@ucdavis.edu

The research leading to this article was supported by Kearney Foundation, as part of the Grant No. 94-19, by the United States Department of Agriculture, as part of the Grant No. 9200544, and by National Science Foundation as part of grant EAR9706623. Valuable comments by anonymous reviewers are acknowledged.

mation from local to global scales and, therefore, hampers our ability to obtain general workable analytical solutions.

Due to the presence of these uncertainties, it has become natural to study the pollution transport problem using stochastic approaches, which supplement the underlying physics via ideas based on probability theory (e.g. Gelhar and Axness, 1983; Dagan, 1984; Mantoglou and Gelhar, 1987; Neuman et al., 1987; Rubin and Gómez-Hernández, 1990; Kabala and Sposito, 1991). This involves propagating the uncertainties in, for example, soil hydraulic properties, into uncertainties in flows and contaminant concentrations, and finding analytical solutions for relevant statistical characteristics of the variables at hand, such as mean, variance, and spatial correlation, under a host of plausible physical and stochastic conditions. Even though the statistical characteristics resulting from the stochastic approaches often provide reasonable pollution transport representations (e.g. Sudicky, 1986), the approaches are also found to possess certain theoretical and practical limitations (e.g. Sposito et al., 1986; Gelhar, 1986), and in some instances give unsatisfactory results (e.g. Black and Freyberg, 1987; Hills et al., 1991). Also, the stochastic approaches typically result in smoothed (even elliptical as in Gaussian plumes) representations of natural patterns, whereas such patterns are often rough and irregular.

In view of these limitations, it seems that progress may be made defining an approach that may capture not only the overall smoothed appearance of natural plumes but also their intricate details. In this regard, the notion of fractal geometry appears to provide a plausible framework for further understanding of the pollution transport process, especially if the dynamics of patterns can be defined in terms of "surrogate" geometric characteristics of the evolving plume.

These ideas may provide a new vision to the problem, as they are consistent with the recently discovered paradigms of chaos and fractals, namely:

(1) details that were thought to be unimportant may play crucial roles in our ability to predict (e.g. Lorenz, 1963; Moon, 1987; Rasband, 1990);
(2) what appears unpredictable and "random" at a local scale could perhaps be explained as part of a global deterministic process (e.g. Lorenz, 1963; Mandelbrot, 1983; Meneveau and Sreenivasan, 1987); and
(3) very complicated processes that were thought to require partial differential equations for modeling may be accurately described by means of very simple deterministic models (e.g. Rasband, 1990; Meneveau and Sreenivasan, 1987; Libchaber, 1982; May, 1976; Feigenbaum, 1980).

The purpose of this study is to propose and test a new approach, based on fractal geometry, to model the dynamics of the pollution transport process. Such an approach is based on the belief that, as concentration profiles (and also soil hydraulic properties) are unique and non-repeating, a proper geometric representation of such patterns would allow capturing their dynamics.

Consistent with the aforementioned paradigms, instead of modeling the statistical characteristics of observed concentrations, this study attempts to represent (or encode) the data sets, gathered at a given time, in their entirety, as projections of stationary measures supported by suitable interpolating functions (e.g. Puente, 1992). Once available patterns are properly encoded, the idea is to look for trends in surrogate parameters (those that define the stationary measures above) so that compact descriptions of the evolving plume and subsequent predictions may be made (e.g. Puente, 1996). That this procedure may indeed provide improved understanding is further explained by the fact that the observed patterns in nature summarize, in a deep sense, all physico-chemical-biological interactions taking place within a heterogeneous porous medium.

The organization of this paper is as follows. First, the fractal geometric procedure is reviewed, identifying the surrogate parameters that need to be specified for a given spatial snapshot of a plume, followed by a description of the study area (the Borden site) and the data sets used. Then, the specific information required regarding the usage of the projection ideas is advanced together with the results obtained using the fractal geometric representation. Finally, the paper ends with conclusions and scope for further study.

2
The fractal-multifractal approach

The basis for this new fractal geometric approach to groundwater contamination dynamics is the representation of concentration patterns (defined in two or more dimensions) as normalized derived distributions obtained by transforming a uniform or a multifractal measure via a fractal interpolating function (Puente, 1992, 1994, 1996a).

Figure 1 illustrates such a representation (bottom), when a fractal interpolating function passing by three points (top) and a uniform measure in the vertical are used. As can be seen, the fractal function maps the vertical into the horizontal plane giving a graph (shaped as a "wire"), which partially fills up three-dimensional space. Such a graph is obtained via arbitrary iterations of two simple mappings guided by a fair coin (with images colored black and gray) and yields, projecting dots into the horizontal plane, the complex histogram (derived measure) below.

In general, a wire passing by $N+1$ points (x_n, y_n, z_n), $n = 0, \ldots, N$, may be built by arbitrarily iterating N affine mappings (Barnsley, 1988), as follows:

$$w_n \begin{pmatrix} x \\ y \\ z \end{pmatrix} = \begin{pmatrix} a_n & 0 & 0 \\ c_n & d_n & h_n \\ k_n & l_n & m_n \end{pmatrix} \begin{pmatrix} x \\ y \\ z \end{pmatrix} + \begin{pmatrix} e_n \\ f_n \\ g_n \end{pmatrix}, \quad n = 1, \ldots, N \tag{1}$$

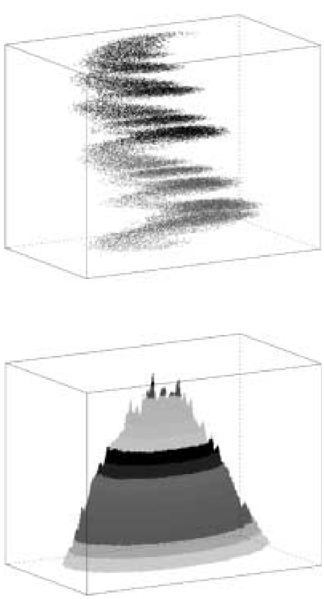

Fig. 1. Construction of a derived measure via the FM approach. The shown wire contains only 10,000 dots but the histogram is made using 1 million values. This wire corresponds to chloride records for day 63 at the Borden site

such that

$$w_n \begin{pmatrix} x_0 \\ y_0 \\ z_0 \end{pmatrix} = \begin{pmatrix} x_{n-1} \\ y_{n-1} \\ z_{n-1} \end{pmatrix}, \quad w_n \begin{pmatrix} x_N \\ y_N \\ z_N \end{pmatrix} = \begin{pmatrix} x_n \\ y_n \\ z_n \end{pmatrix}, \tag{2}$$

with the sub-matrix

$$A_n = \begin{pmatrix} d_n & h_n \\ l_n & m_n \end{pmatrix} \stackrel{\text{def}}{=} \begin{pmatrix} r_n^{(1)} \cos\theta_n^{(1)} & -r_n^{(2)} \sin\theta_n^{(2)} \\ r_n^{(1)} \sin\theta_n^{(1)} & r_n^{(2)} \cos\theta_n^{(2)} \end{pmatrix} \tag{3}$$

having a norm less than one (i.e. with the maximum eigenvalue of $A_n^{\mathrm{T}} A_n$ being less than one).

Under these conditions, unique stationary measures dx and dyz are obtained in x (the vertical) and over (y, z) (the horizontal), irrespective of the actual path of iterations taken (Puente, 1994a, b). dyz is the derived measure found transforming dx via the unique fractal interpolating function f given by the iterations, whose graph $G = \{(x, y, z) = (x, f(x))\}$ satisfies $G = \bigcup_{n=1}^{N} \omega_n(G)$ (Puente, 1994a) and has a fractal dimension ranging from 1 to 3 (Barnsley, 1988; Puente and Klebanoff, 1994).

At the end, the construction leaves the four coefficients in matrix A_n free, with a_n, c_n, k_n, e_n, f_n, and g_n determined in terms of the scalings $r_n^{(1)}, r_n^{(2)}$, rotations $\theta_n^{(1)}, \theta_n^{(2)}$, and the $N + 1$ interpolating points. By varying such parameters and the coin (dice) bias used to compute mapping iterations, a wide range of deterministic derived measures dyz may be obtained, ranging from unsmooth patterns to elliptical Gaussian distributions. Such sets turn out to be functionally linked (via the fractal functions) to either uniform or multifractal measures dx induced by the iterations over x (Puente, 1992, 1994a). As multifractals have been found related to turbulence (Meneveau and Sreenivasan, 1987), this functional link provides a "physical" interpretation of the derived histograms as "reflections" of turbulence.

In what follows we shall show how to find fractal-multifractal representations for normalized concentration profiles gathered in practice.

3
Study area and data used

The present study investigates the suitability of the fractal-multifractal approach to represent vertically averaged two-dimensional concentration patterns measured at the Borden site in Ontario, Canada. Comprehensive descriptions of the climate, geology, and hydrology of such a site are presented in a number of studies (e.g. MacFarlane et al., 1983; Mackay et al., 1986) and, therefore, are not reported herein. Some of the important characteristics of the site are:

(a) it is a relatively homogeneous medium-to fine-grained sandy unconfined aquifer, containing thin lenses extending from 2 to 5 m;
(b) its water table depth fluctuates over the year within the range 0.5–1.0 m below surface;
(c) its aquifer is approximately 10 m thick in the vicinity of the experimental site, underlain by a thick silty clay aquitard; and
(d) it contains a plume of contaminants, predominantly inorganic, originating at a landfill located approximately 400 m south of the experimental site, within the bottom 2–3 m of the aquifer.

This work relies on the tracking of chloride and bromide tracers, injected at the site on August 23, 1982, in order to study contamination dynamics (e.g. Mackay et al., 1986). Specifically, this study employs the concentration profiles observed at the site on ten dates spanning 647 days after injection: days 1, 9, 29, 43, 63, 259, 332, 381, 462 and 647, defining contours for such conservative tracers via a two-step procedure, similar to the one adopted by Freyberg (1986), as follows. Given raw data defined over the vertical at several locations, a trapezoidal quadrature integration is used first to define vertically averaged estimates at such a location. Then, a horizontal interpolation scheme, based on a grid-based contouring and a three-dimensional surface plotting graphics program (SURFER version 4.15, 1994), is used together with ordinary Kriging, in order to define "observed" concentrations over an arbitrarily selected 25×25 rectangular grid containing the extent of the plume. Given that the FM methodology requires "probability" patterns, these data sets are finally normalized such that their masses add up to one.

As other investigators have considered the Borden site records in a variety of studies, the following remarks are of relevance:

(a) since the method used to interpolate horizontally is not exactly the same as the ones employed in earlier studies (e.g. Freyberg, 1986; Barry and Sposito, 1990; Rajaram and Gelhar, 1991), the "observed" patterns described using the FM procedure do not exactly match the concentration patterns used by those studies. The overall shapes and trends, however, are indeed quite similar; and

(b) issues pertaining to the possible errors that might have resulted in the sampling of the plumes are not considered here (e.g. Rajaram and Gelhar, 1991). As variations of the recovered masses, obtained from the present study, are comparable to the results reported by Freyberg (1986), it is assumed that the normalized data sets are indeed representative of the successive behaviors of the conservative plumes.

Since it is observed that the plumes of chloride and bromide basically exhibit very similar evolutions, only the results for chloride are presented herein.

4
Data processing via the FM approach

For each of the ten frames of chloride used in this study, a three-dimensional wire is sought such that its projection (based on a uniform measure over the vertical, i.e. having iterations guided by a fair coin) would closely reproduce the desired patterns, with the x axis lying perpendicular to the plane where concentrations are defined, i.e. y–z.

Although alternative derived measures can be found by varying the surrogate parameters of a fractal interpolating function f, there are, unfortunately, no simple analytical formulas that give either the joint derived measure dyz, or its most common statistics, in terms of these parameters. This implies that an inverse problem needs to be solved numerically for a given spatial set.

It has been our experience that developing a catalog of patterns similar to the ones being sought represents an important starting step for solving such an inverse problem. By looking at pages on such an interactive catalog, one arrives at suitable initial conditions that may be used together with sophisticated searching procedures. In all cases to be reported, "optimal" (local) wires are obtained by minimizing squared differences between real and FM outcomes in terms of a combination of classical statistical attributes, commonly used in stochastic transport theories. These statistical qualifiers include the first four order moments for concentration data sets when seen from both the space axes (y and z) and the concentration axis, and the sum of squared point by point differences between observed and fitted plumes (over the 25×25 grid). In all cases, the actual objective function has a weighted sum of such attributes so that all terms have relatively the same importance.

Given the nature of the complicated numerical search, a two-step optimization procedure is considered. During the first stage, preliminary parameters are found, by employing the multidimensional simplex method (Press et al., 1989) starting the procedure using parameters from the aforementioned catalog. Then, these parameters are used as seeds for more sophisticated searching procedures, which include simulated annealing (Otten et al., 1989) and/or shuffled complex evolution (Duan et al., 1992).

5
Results and discussion

The results obtained using the FM methodology for the chloride sets at the Borden site are presented next.

5.1
Plume geometry and low order statistics

As may be seen in Figs. 2 and 3, including "real" (left) and FM fitted (right) profiles for eight of the ten days considered, the fractal geometric approach provides a reasonable model for the vertically-averaged chloride plume at the Borden site [with the axes (Y, Z) corresponding to (Y, X), as used by Freyberg (1986)]. This may be noted by an approximate visual agreement that translates into close preservation of the plume's center of mass, its spread, and some of its geometric details.

That the FM approach gives suitable representations for all dates may be further illustrated by Table 1, that presents low order moment information for real and fitted profiles. The table includes: (i) the center of mass on both spatial axes ($\bar{y}$ and $\bar{z}$), (ii) the standard deviations on both spatial axes (σ_y and σ_z) and the correlation coefficient (ρ), (iii) the coefficients of skewness and kurtosis on both spatial axes (γ_y, γ_z, κ_y and κ_z), and (iv) the standard deviation (σ_c), the coefficient of skewness (γ_c), and the coefficient of kurtosis (κ_c) for the data obtained from the concentration axis.

As the table indicates, although on some days the characteristics of the plume are not as well preserved as in others, the first and second order moments in all of the three axes are generally in very good agreement. For instance, the center of mass has been fitted with errors that are less than 10% on all the days and the standard deviations contain errors that exceed 15% only for σ_y on days 259 and 332.

5.2
Plume parameterization

All the FM representations shown in Figs. 2 and 3 are obtained by employing a minimal scheme, consisting of a fractal interpolating function passing by only three points in three-dimensional space. As all dates share equally the set 0, 0.5 and 1 in x, chloride profiles for all dates may be interpreted as a "projection" of a uniform measure supported by a three-dimensional wire, a set that is parameterized by the interpolating points in y and z and the scalings and rotations of two affine mappings (Eq. (2)).

Figure 4 presents the "best" FM surrogate parameters found for the ten chloride patterns from the measurements at the Borden site. As can be seen, the

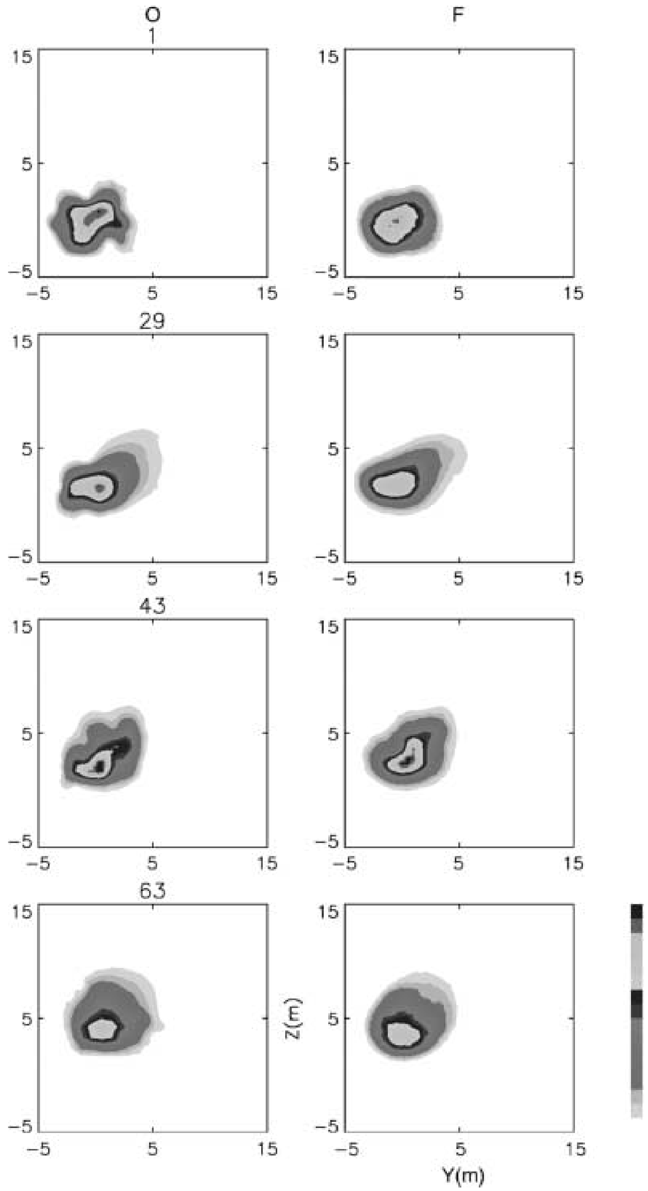

Fig. 2. Measured (left) and FM fitted (right) chloride at the Borden site for days 1, 29, 43, and 63 after injection. The gray-scale bar varies between zero (bottom) and 248.95 mg/L (top)

quantities that change the most are the coordinates of the interpolating points both in y and in z, which do so in a “linear” fashion. Moreover, these parameters are closely related to the movement and growth (dispersion) of the plume, for as the plume moves and grows, so it happens with the y–z coordinates, which preserve the higher dispersion in z than in y, as seen in Figs. 2 and 3. As shown in Fig. 5, the interpolating points are indeed nicely linked to the evolution of the plumes’ center of mass and dispersion.

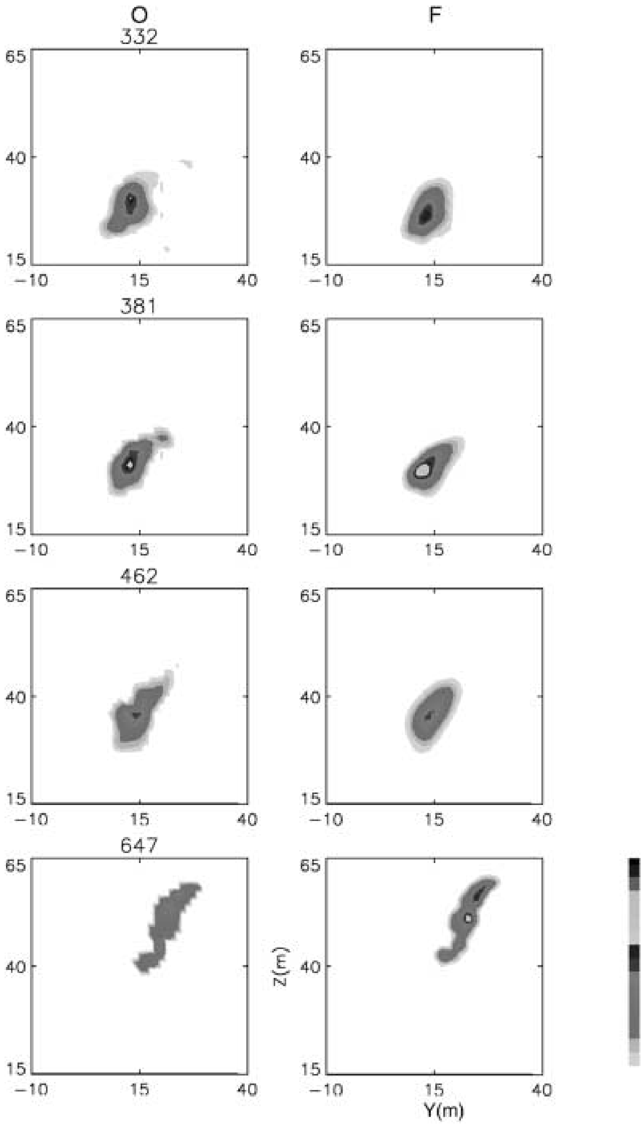

Fig. 3. Measured (left) and FM fitted (right) chloride at the Borden site for days 332, 381, 462, and 647 after injection. The gray-scale bar varies between zero and 248.95 mg/L (top)

As can be appreciated in Fig. 4, the scalings are the least stable of all the surrogate parameters. Even though the values of all of them are relatively close to their maximal value of 1, they exhibit clear oscillations during the first few days after injection and they do not show a definite trend during the latter days. On the other hand, the rotations, despite variations during the first few days, show clear signs of stabilization, indicating that the affine mappings may be properly defined with a single rotation per mapping.

As revealed by Puente and Klebanoff (1994), when the magnitude of all scaling parameters tends to 1 and when only one rotation is required per mapping, the derived bivariate measures become Gaussian. The high values of the magnitude of the scaling parameters, shown in Fig. 4, hence suggest that the

Table 1. Lower order moments for chloride at the Borden site (Observed and FM Fitted)

Day	$\bar{y}$	$\bar{z}$	σ_y	σ_z	ρ	γ_y	γ_z	κ_y	κ_z	σ_c	γ_c	κ_c
	Measured											
1	0.42	0.47	1.65	1.34	0.13	0.08	0.03	2.28	2.52	0.0021	1.27	3.37
9	0.73	0.63	1.86	1.12	0.10	0.20	0.26	2.23	2.72	0.0022	1.34	3.55
29	1.45	3.07	2.10	1.59	0.47	0.36	0.76	2.51	3.54	0.0025	1.94	6.07
43	1.54	4.10	1.73	1.62	0.34	−0.03	0.47	2.19	2.60	0.0024	1.72	5.26
63	1.39	5.19	1.79	1.68	0.15	0.25	0.51	2.42	2.62	0.0057	4.31	22.72
259	11.68	23.36	3.62	2.70	0.47	2.06	−0.10	8.75	2.46	0.005	3.82	18.06
332	15.16	29.09	3.38	3.78	0.50	1.01	0.28	5.81	2.84	0.0041	3.13	13.02
381	15.72	32.42	3.17	3.38	0.66	0.62	−0.03	3.08	2.32	0.0052	3.84	18.34
462	16.84	38.51	3.19	4.16	0.63	0.33	0.10	2.69	2.49	0.0046	3.33	14.41
647	23.68	52.86	3.18	5.65	0.83	0.11	−0.31	2.54	1.90	0.0051	3.02	10.70
	Fitted											
1	0.45	0.46	1.63	1.33	0.12	0.07	0.08	2.28	2.47	0.0023	1.50	4.21
9	0.73	0.66	1.80	1.16	0.09	0.11	0.22	2.27	2.64	0.0028	2.01	6.01
29	1.41	3.03	2.05	1.50	0.38	0.32	0.40	2.62	3.00	0.0029	2.27	7.51
43	1.56	4.07	1.73	1.57	0.33	−0.06	0.34	2.57	2.54	0.0032	2.52	8.95
63	1.35	5.21	1.75	1.68	0.17	0.24	0.43	2.45	2.66	0.0032	2.64	9.80
259	10.93	23.10	2.37	2.58	0.47	0.37	−0.21	2.61	2.63	0.0054	4.22	21.6
332	15.08	29.06	2.84	3.52	0.32	0.09	0.14	2.84	2.52	0.0055	4.61	25.76
381	15.87	32.52	3.13	3.10	0.57	0.45	0.11	3.04	2.60	0.0046	3.66	19.72
462	16.75	38.43	3.06	4.03	0.54	0.16	−0.11	2.82	2.71	0.0042	3.42	15.11
647	23.89	53.10	3.06	5.50	0.82	−0.02	−0.24	2.74	2.02	0.0040	2.78	9.99

Note: $\bar{y}$, $\bar{z}$, σ_y, σ_z in meters; σ_c in dimensionless concentrations

chloride patterns for the Borden site are "fairly" elliptical. Notice that the constancy of the rotations, especially after the plume samples larger regions in space, is consistent with the fact that the center of mass of the plume travels along a line in space corresponding to the longitudinal axis of the plume (Freyberg, 1986).

The clear trends in coordinates and rotations, and also the high fitted scalings, seem to indicate the possibility of building a model on surrogate parameter space for representing the evolving plume and also for subsequent predictions. Such predictions, based on the belief that the observed trends in surrogate parameters persist even as the plume samples regions of larger extent, may give appropriate reflections of what is happening inside the porous medium. Whether or not this idea can provide reasonable predictions is illustrated in a companion article (Puente et al., 2001). It is relevant to note, however, that the shape of a plume varies as it samples larger heterogeneities within the soil and, therefore, predictions using the FM approach (or any other procedure for that matter) could be quite wrong if the medium properties change.

5.3
Common plume characteristics

Plots of the center of mass of the FM fitted vertically averaged chloride snapshots in the horizontal y–z plane (not included here) reveal that they follow a nearly linear trajectory over the duration of the Borden site experiment, as found with the records. The best fit for the FM chloride plume, obtained with an angle of 25° clockwise from the z axis, is in good agreement with the 25.5° reported by Freyberg (1986). Also, the estimated mean velocity of the center of mass of the FM fitted plume is 0.092 m/day, which is very close to 0.091 m/day found by Freyberg (1986).

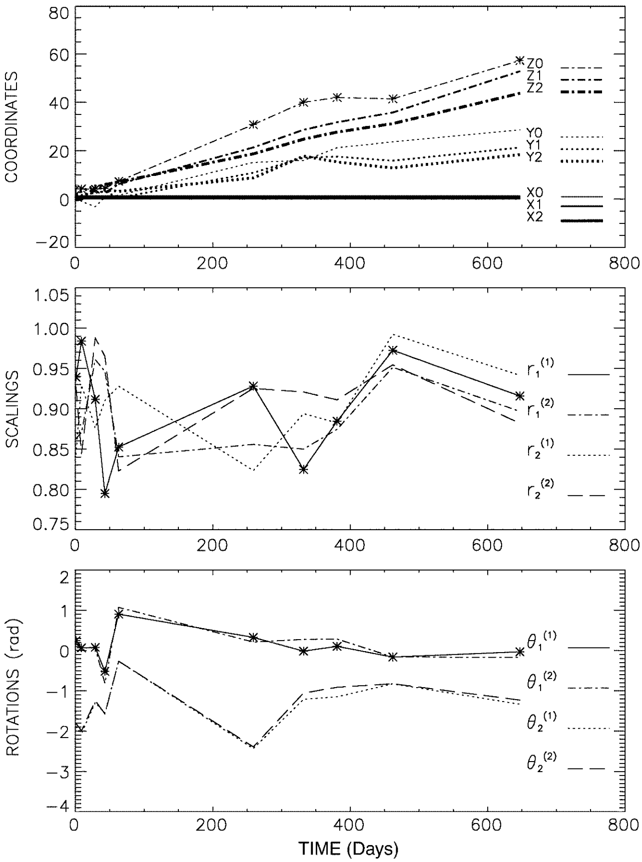

Fig. 4. Evolution of FM surrogate parameters for chloride at the Borden site

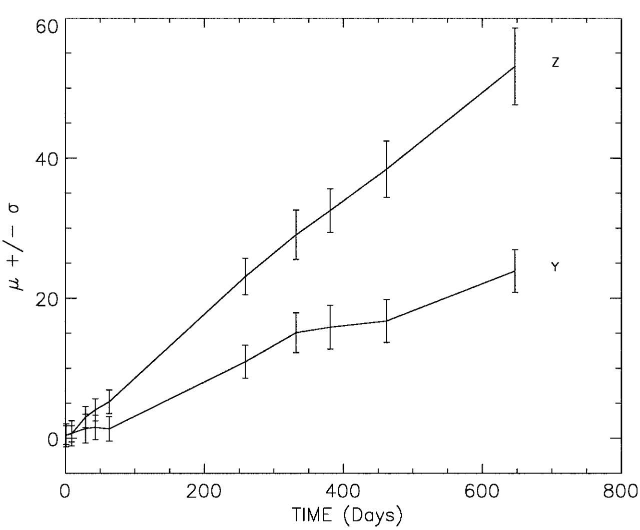

Fig. 5. Evolution of the center of mass ± one standard deviation for chloride at the Borden site

Table 2. Rotated second order moments for chloride at the Borden site (Observed, FM Fitted, and as reported by Freyberg, 1986)

Day	Measured			Fitted			Freyberg		
	σ_L^2	σ_T^2	Cov (L,T)	σ_L^2	σ_T^2	Cov (L,T)	σ_L^2	σ_T^2	Cov (L,T)
1	2.18	2.33	0.54	2.13	2.30	0.51	2.10	2.40	0.50
9	1.81	2.91	0.98	1.83	2.76	0.85	1.70	2.40	0.70
29	4.07	2.87	1.73	3.63	3.18	1.69	2.50	2.60	0.90
43	3.42	2.20	0.75	3.30	2.21	0.78	4.40	2.70	1.20
63	3.24	2.79	0.44	3.25	2.64	0.41	4.40	2.40	1.10
259	11.85	8.55	5.18	8.67	3.60	1.45	17.80	4.40	3.70
332	18.67	7.04	3.01	14.07	6.39	0.40	–	–	–
381	16.60	4.88	4.02	13.88	5.53	3.62	20.60	4.40	3.90
462	22.43	5.04	2.64	20.11	5.49	1.65	27.80	5.50	2.10
647	39.45	2.58	1.23	37.09	2.52	0.87	51.50	5.50	3.00

Note: σ_L^2, σ_T^2, in squared meters

Table 2 compares the second order moments for the chloride plume as found in the present study and in others, when the set of coordinates is aligned with the straight line that describes the time evolution of the center of mass of the plume (i.e. a rotation of $-25.0°$). As can be seen, the values obtained from the FM approach are in good agreement not only with the observed values but also with the corresponding moments reported by Freyberg (1986). This may be seen graphically in Fig. 6 that presents the plume's spatial moments of order two. This includes moments for observed sets (asterisks), and FM fitted patterns (diamonds), as well as values reported by Freyberg (1986) (squares) and best regression lines through FM fitted moments (solid line).

From these figures, the apparent dispersivities for the three components of the covariance tensor give (in meters): (a) longitudinal $A_L = 0.321$, (b) transverse $A_T = 0.026$, and (c) longitudinal-transverse $A_{L,T} = 0.017$, which favorably compare with the observed values of, in order, 0.311, 0.018, and 0.017. As may be verified, these FM values are also very close to those reported by Freyberg (1986). These observations reiterate that the FM approach is indeed capable of capturing the most important characteristics of the plume, as used in stochastic theories.

To illustrate further the closeness achieved with the FM methodology in spatial moments, Fig. 6 also includes covariance tensor values as implied by the two-dimensional stochastic transport model of Dagan (1984) (broken line), i.e.

$$\sigma_L^2(t) = 1.8 + 0.74\sigma_{\ln K}^2 l_{\ln K}^2 \left\{ 2\frac{t}{T} + \frac{3}{2} + 3\left[Ei\left(-\frac{t}{T}\right) - \ln\left(\frac{t}{T}\right) - \gamma \right] + 3\frac{e^{-t/T}[1 + t/T] - 1}{[t/T]^2} \right\} \tag{4}$$

$$\sigma_T^2(t) = 2.6 + 0.74\sigma_{\ln K}^2 l_{\ln K}^2 \left\{ -\frac{3}{2} - \left[Ei\left(-\frac{t}{T}\right) - \ln\left(\frac{t}{T}\right) - \gamma \right] - 3\frac{e^{-t/T}[1 + t/T] - 1}{[t/T]^2} \right\} \tag{5}$$

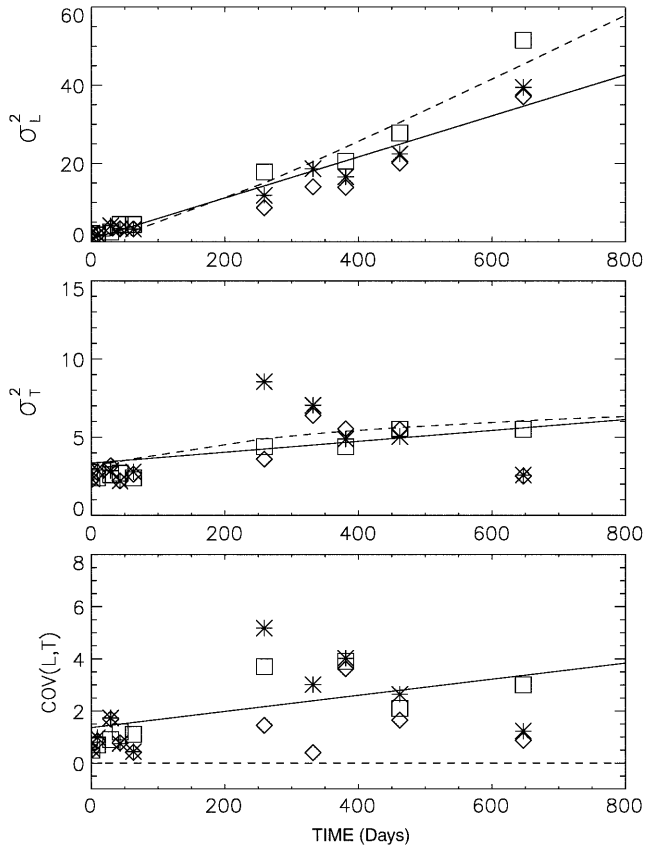

Fig. 6. Spatial covariance tensors for chloride at the Borden site. Observed records (asterisks), FM fitted plumes (diamonds), best linear line via FM fitted values (solid line), as reported by Freyberg (1986) (squares), via Dagan's model (1984) (broken line). **a** Longitudinal component, **b** Transverse component, **c** Covariance

$$\sigma_{L,T}(t) = 0 \quad , \tag{6}$$

where $\sigma^2_{\ln K}$ and $l_{\ln K}$ are, respectively, the variance and correlation scale of the logarithm of the hydraulic conductivities for the medium; $\gamma = 0.5772\ldots$ is Euler's constant; $Ei(.)$ is the exponential integral; and $T = l_{\ln K}/|U|$ is a characteristic time.

As may be seen in Fig. 6, and as previously reported by Freyberg (1986) (but including the bromide observation at day 1038 after injection), Dagan's model nicely captures both longitudinal and transverse directions, and closely fits the FM generated plume.

As first and second order moments only provide a partial description of the spatial patterns, Fig. 7 includes the entropy and dilution index (an entropy related measure), (Thierrin and Kitanidis, 1994), that depend on the overall shape of the records, either real or FM fitted. As may be seen, these quantities defined by:

$$\text{Entropy1} = \sum_i \sum_j C_{i,j} \ln C_{i,j} \tag{7}$$

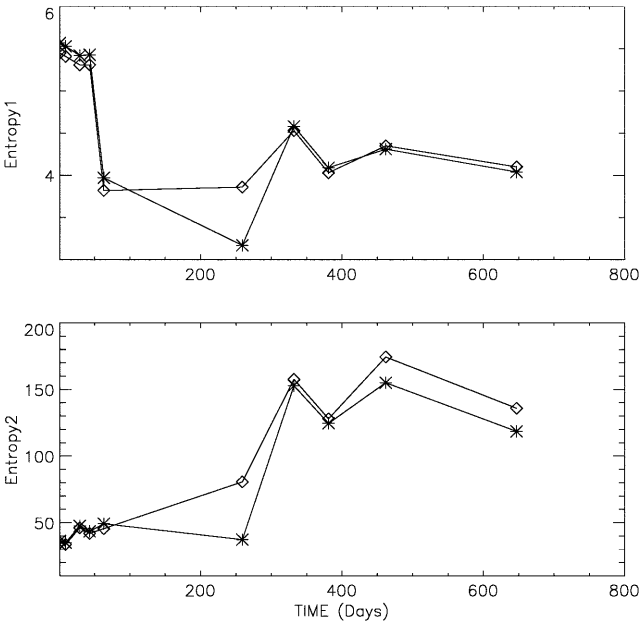

Fig. 7. Evolution of entropy and dilution index for chloride at the Borden site. Observed records (asterisks), FM fitted plumes (diamonds)

$$\text{Entropy2} = \Delta A \exp\left[-\sum_i \sum_j C_{i,j} \ln C_{i,j}\right] \qquad (8)$$

where $C_{i,j}(t)$ are the normalized concentrations over the 25×25 grid at every time; and ΔA is the size of the elementary area being used (i.e. the product of horizontal lengths each divided by 24), also yield close agreement between real and fitted plumes (except for day 259), which further corroborate the ability of the fractal geometric approach in preserving the natural patterns at hand.

6
Conclusions and scope for further study

The possibility of modeling the dynamics of groundwater contamination via a fractal geometric framework has been investigated. Based on the concept of projections off fractal interpolation functions, this study has shown that it is indeed possible to capture the plume geometry of conservative tracers, chloride and bromide gathered at the Borden site, leading to a vantage point (in surrogate fractal geometric space) that enables us to view the evolution of such plumes in a wholistic fashion.

It was found that surrogate parameters for the cases considered exhibited clear trends, as follows:

(a) the interpolating points in y–z grew linearly, following the evolution of the plume's center of mass;
(b) the scalings showed no definite trends and gave high values (above 0.8) that reflect the "elliptical" nature of the patterns; and
(c) the rotations evolved by couples in a fairly constant fashion, leading to one such parameter per affine mapping.

These observations suggest that it may be possible to arrive at a dynamic description of the Borden site plume without the need of partial differential equations. Details of the application of such ideas in order to predict the evolving plumes are reported in a companion paper (Puente et al., 2001).

Whether or not the fractal-multifractal methodology may be fully applicable to model contamination dynamics at other sites is uncertain at this stage. As illustrated in this work, solution of a non-trivial inverse problem is required and the approach turns out to be useful only in the presence of well established trends in surrogate parameter space. However, our results illustrate the flexibility of the geometric approach in capturing natural geometries, and hence encourage testing it under a variety of circumstances that should also include numerically generated plumes. Also, it should be noted that extension of the ideas to even higher dimensions is straightforward, and therefore the potential for geometrically representing full three-dimensional plumes exists.

Even though a plume representation based on twelve surrogate parameters (six coordinates, four scalings and two rotations) may appear to be not parsimonious, it should be noted that the fractal geometric approach used herein attempts to capture "whole" data sets rather than only a few statistical descriptions of the records. It should also be noted that the present deterministic approach is different from other fractal-based methodologies that attempt to model some statistical characteristics of the porous medium, e.g. power law variograms (Neuman, 1990) or autocorrelations for fractal or multifractal soil matrices (Wheatcraft and Tyler, 1988; Rieu and Sposito, 1991).

References

Barnsley MF (1988) Fractals Everywhere, Academic Press, New York

Barry DA, Sposito G (1990) Three-dimensional statistical moment analysis of the Stanford/Waterloo Borden tracer data. Water Resour. Res. 26(8): 1735–1747

Black TC, Freyberg DL (1987) Stochastic modeling of vertically averaged concentration uncertainty in a perfectly stratified aquifer. Water Resour. Res. 23(6): 997–1004

Dagan G (1984) Solute transport in heterogeneous porous formations. J. Fluid Mech. 145: 151–177

Duan Q, Gupta VK, Sorooshian S (1992) Effective and efficient global optimization for conceptual rainfall–runoff models. Water Resour. Res. 28(4): 1015–1031

Feigenbaum MJ (1980) Universal behavior in nonlinear systems. Los Alamos Science, Summer 4–27

Freyberg DL (1986) A natural gradient experiment on solute transport in a sand aquifer. 2. Spatial moments and the advection and dispersion of nonreactive tracers. Water Resour. Res. 22(13): 2031–2046

Gelhar LW (1986) Stochastic subsurface hydrology: From theory to applications. Water Resour. Res. 22(9): 135S–145S

Gelhar LW, Axness CL (1983) Three dimensional stochastic analysis of macrodispersion in aquifers. Water Resour. Res. 19(1): 161–180

Hills RG, Wierenga PJ, Hudson DB, Kirkland MR (1991) The second Las Cruces trench experiment: Experimental results and two-dimensional flow predictions. Water Resour. Res. 27(10): 2707–2718

Kabala ZL, Sposito G (1991) A stochastic model of reactive solute transport with time-varying velocity in a heterogeneous aquifer. Water Resour. Res. 27(3): 341–350

Libchaber A (1982) Convection and turbulence in liquid helium I. Physica B 109/110: 1583–1589

Lorenz EN (1963) Deterministic nonperiodic flow. J. Atmos. Sci. 20: 130–141

MacFarlane DS, Cherry JA, Gillham RW, Sudicky EA (1983) Migration of contaminants in groundwater at a landfill: A case study, 1, Groundwater flow and plume delineation. J. Hydrol. 63: 1–29

Mackay DM, Freyberg DL, Roberts PV, Cherry JA (1986) A natural gradient experiment on solute transport in a sand aquifer. 1. Approach and overview of plume movement. Water Resour. Res. 22(13): 2017–2029
Mandelbrot BB (1983) The Fractal Geometry of Nature, Freeman, San Francisco
Mantoglou A, Gelhar LW (1987) Stochastic modeling of large-scale transient unsaturated flow systems. Water Resour. Res. 23(1): 37–46
May RM (1976) Simple mathematical models with very complicated dynamics. Nature 261: 459–467
Meneveau C, Sreenivasan KR (1987) A simple multifractal cascade model for fully developed turbulence. Phys. Rev. Lett. 59: 1424–1427
Moon FC (1987) Chaotic Vibrations, Wiley, New York
Neuman SP (1990) Universal scaling of hydraulic conductivities and dispersivities in geologic media. Water Resour. Res. 26(8): 1749–1758

Neuman SP, Winter CL, Newman CM (1987) Stochastic theory of field-scale fickian dispersion in anisotropic porous media. Water Resour. Res. 23(3): 453–466
Otten RHJM, van Ginneken LPPP (1989) The Annealing Algorithm, Kluwer Academic Publishers, Boston
Press WH, Flannery BP, Teukolsky SA, Vetterling WT (1989) Numerical Recipes, Cambridge University Press
Puente CE (1992) Multinomial multifractals, fractal interpolators and the Gaussian distribution. Phys. Lett. A 161: 441–447
Puente CE (1994a) A fractal-multifractal approach to geostatistics. In Dimitrakapoulos R (ed.) Geostatistics for the Next Century, pp. 476–487 Kluwer Academic Publishers, Dordrecht
Puente CE (1994b) Deterministic fractal geometry and probability. Int. J. Bifurcation and Chaos 4(6): 1613–1629
Puente CE (1996) A new approach to hydrologic modeling: Derived distributions revisited. J. Hydrol. 187: 65–80
Puente CE, Klebanoff AD (1994) Gaussians everywhere. Fractals 2(1): 65–79
Puente CE, Robayo O, Sivakumar B (2001) A fractal-multifractal approach to groundwater contamination. 2. Predicting conservative tracers at the Borden site. Stoc. Envir. Res. Risk Asses. 15: 372–383
Rajaram H, Gelhar LW (1991) Three-dimensional spatial moments analysis of the Borden tracer test. Water Resour. Res. 27(6): 1239–1251
Rasband SN (1990) Chaotic Dynamics of Nonlinear Systems, John Wiley & Sons, New York
Rieu M, Sposito G (1991) Fractal fragmentation soil porosity, and soil water properties. 1. Theo. Soil Scie. Soci. Ame. J. 55(5): 1231–1238
Rubin Y, Gómez-Hernández JJ (1990) A stochastic approach to the problem of upscaling of conductivity of disordered media: Theory and unconditional simulations. Water Resour. Res. 26(4): 691–701
Sposito G, Jury WA, Gupta VK (1986) Fundamental problems in the stochastic convection dispersion model of solute transport in aquifers and field soils. Water Resour. Res. 22(10): 77–88
Sudicky EA (1986) A natural gradient experiment on solute transport in a sand aquifer: Spatial variability of hydraulic conductivity and its role in the dispersion process. Water Resour. Res. 22(13) 2069–2082
SURFER for Windows, User's Guide (1994) Golden Software Inc., Golden, Colorado
Thierrin J, Kitanidis PK (1994) Solute dilution at the Borden and Cape Cod groundwater tracer tests. Water Resour. Res. 30(11): 2883–2890
Wheatcraft SW, Tyler SW (1988) An explanation of scale-dependent dispersivity in heterogeneous aquifers using concepts of fractal geometry. Water Resour. Res. 24(4): 566–578